OPERATION OF THE APEX PHOTOINJECTOR ACCELERATOR AT 40 MEV*

D. W. Feldman, S. C. Bender, D. A. Byrd, B. E. Carlsten, J. W. Early, R. B. Feldman, J. C. Goldstein,
R. L. Martineau, P. G. O'Shea, E. J. Pitcher, M. J. Schmitt, W. E. Stein, M. D. Wilke, and T. J. Zaugg
Los Alamos National Laboratory, MS-J579
Los Alamos, NM 87545

ABSTRACT

We have successfully operated the photoinjector and rf linear accelerator for the Los Alamos APEX free electron laser(FEL) at design energy, average macropulse current, and emittance. The accelerator, which operates at 1.3 GHz, consists of a 6 MeV photoinjector and three standing-wave structures with a total beam energy of 40 MeV.

This paper presents performance characteristics of the APEX system. The results show that this technology is capable of providing reliable, high-peak current, ultra-high brightness electron beams.

INTRODUCTION

Accelerator research in the Los Alamos free electron laser program has focused on the theoretical and experimental development of high-current, low-emittance systems that can serve as drivers for high-power, high-efficiency FEL's. This research has led to the construction of an accelerator and beamline based on a photoelectric injector.

This technology was shown in earlier LANL experiments and simulations to be superior to conventional injectors in high-current regimes[1,2]. As a result, the photoinjector is now becoming the design of choice for high-current, low-emittance devices.

We have successfully operated the accelerator for the Los Alamos APEX free-electron laser facility at its design parameters, and measured a number of relevant characteristics, including emittance, peak current, energy spread, and wakefields.

This paper presents a brief description of the APEX system's components and provides an update on research completed so far.

COMPONENTS

Figure 1 shows the APEX systems layout. The FEL components will not be discussed here.

Photoinjector

The photoinjector/accelerator consists of six high-gradient accelerating cells with on-axis coupling cells between them. The accelerator operates in a $\pi/2$ mode at 1.3 GHz and 6-7 MeV. The first accelerating cell is a half cell with a photocathode on the half-plane surface. The photoinjector/accelerator is followed by three more accelerator structures to bring the beam energy up to 40 MeV. The four accelerator structures are powered by four Thompson modulation-anode klystrons. The electron source is a photocathode consisting of a multi-alkili film that is produced *in situ* and irradiated by a frequency doubled Nd:YLF laser.

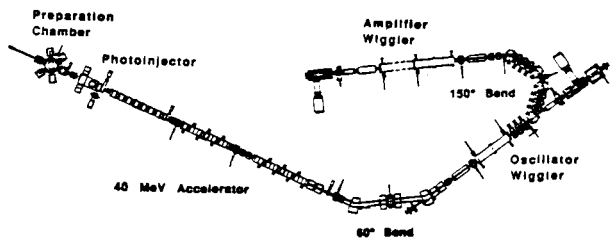

Fig. 1 APEX Accelerator and Beamline

Table I shows the design parameters for the APEX accelerator.

TABLE I
Design Parameters for APEX Accelerator

Energy,	40 MeV
$\Delta E/E$	0.24%
Emittance (rms)	$\leq 13\pi$ mm-mr @350 A
	3.3π mm-mr@130 A
Micropulse Charge	0-5 nC
Micropulse Width	7-16 ps
Micropulse Rep. Rat	21.7 MHz
Peak Current	0-350 A
Macropulse Length	0-100 μs
Normalized Brightness(rms)	3×10^{12} A/(m-rad)^2
	@ 135 A

We have met these design goals.

Beamline

The beam transport line was modified to minimize the discontinuities seen by the electrons between the photocathode and the wiggler. Calculations indicate that the expected emittance of the e-beam will not be appreciably degraded by the beam transport [2].

For the measurements reported here, we operated the beamline as far as the first spectrometer after the wiggler. The remaining beamline will consist of a 150° bend and a second

*Work supported and funded by the US Department of Defense, Army Strategic Defense Command, under the auspices of the US Department of Energy

wiggler (Fig. 1). In future experiments, we will use this arrangement to test the validity of transport codes, to demonstrate bunching in the bend, and to demonstrate the operation of a single accel-erator master oscillator-power amplifier [3].

Photocathode

The photocathode is formed on a molybdenum plug which is pulled back from the first cell of the photoinjector/accelerator into a preparation chamber. The cathode is prepared by successive evaporation of antimony, potassium, and cesium.

Photocathode Drive Laser

Electrons are produced from the photocathode by illumination from a frequency-doubled Nd:YLF laser operating at 527 nm with nominal pulse-width of 10 ps.

Diagnostics

Beam profiles are observed by optical transition radiation emitted at aluminum surfaces of insertable screens. In our experiments, we used Cerenkov light with a streak camera to measure variations in e-beam pulse width and transit time. The streak camera was also used to study micropulse wakefield effects.

We used a spectrometer at the end of the beamline to measure energy and energy spread. We monitored the amplitude and phase of the rf voltages in each of the accelerator tanks for each macropulse.

MEASUREMENTS AND RESULTS

Component Operation

Injector. We observed three unanticipated effects in the newly designed injector/accelerator: (1)oscillations in the amplitude and phase of the rf fields in the accelerator caused by multipactoring, (2)field emission from the low work function photocathode caused by the high field gradients in the first cell, and (3)focusing effects caused by the on-axis coupling slots. These effects and their impact on operations are described in more detail by Feldman et. al. [4].

Photocathode. The quantum efficiency of the photocathodes as formed was typically ≈5-10% under the 527 nm excitation of our frequency-doubled Nd:YLF drive laser with a typical variation of about 10%.

Under our operating conditions,(i.e., 0.1A average macropulse current and $\approx 10^{-4}$ duty cycle) the cathode lifetime was 5-15 hours. The cathode lifetime is strongly correlated with the pressure in the accelerator during operation.

Drive laser. The drive laser pulse width at the cathode was typically 10-12 picoseconds with micropulse energy output at the laser of 10 μJ. The measured phase and amplitude jitter[5] were low enough that the measured emittance and energy spread were not compromised by the drive laser.

Rf controls. The present rf controls maintain the phase and amplitude stability of the rf fields to 1° of phase and 0.5% in amplitude over a macropulse width of 20 μs. Calculations indicate that the rf stability is not a limiting factor for our operation.

Beam Measurements

Energy spread. The fractional energy spread of a 20 μs macropulse was measured to be 0.24% FWHM at a micropulse charge of 5 nC. The measurement agrees with simulations[2] that model the accelerator.

Pulse stretching. Using the streak camera,we measured the stretching of the micropulse from the initial pulse width produced at the cathode and the variation of transit time through the accelerators as a function of the phase of the drive laser pulse with respect to the rf accelerating fields and the micropulse charge. These measurements, and the results of ref. [6], agreed well with the PARMELA simulations, giving added confidence in the codes used.

Space charge limited emission. We observed space charge limited emission from the photocathode at high current densities. At our nominal operating condition of about 300 A/cm^2, we are in the emission limited regime for injection over most of the rf cycle. However, we can reach high enough current densities(>6 kA/cm^2) to be in the space charge limited regime for the full 25 MeV/m field strength. Both a simple Child-Langmuir law and PARMELA describe the observed behavior over large phase angles.

Emittance. We give e-beam emittances for purposes of comparison in terms of rms values. We measured all beam profiles in terms of full-width at half maximum intensity and calculated experimental rms value by assuming a Gaussian shape. We measured emittance with the two screen technique, with optical transition radiation interferometry, and with the more standard quad-scan method.[7].

If a high-current beam traverses a part of the transport line or a bend off center, strong transverse wakefields can be generated that produce different deflections for different parts of the micropulse, causing different parts of the micro-pulse to focus differently. As a result, emittance is increased. Misalignment of quads also causes an increase in emittance. Simulations have shown that the most sensitive regions are in the accelerator structures and in the bends. Therefore we took great care to align the accelerators and beamline components to the best of our ability, using optical tooling and the pulsed-wire method for the quads.

Figure 2 shows the results of emittance measurements before the 60° bends . The two curves in fig. 2 are calculated from PARMELA. The calculation of the lower curve assumed

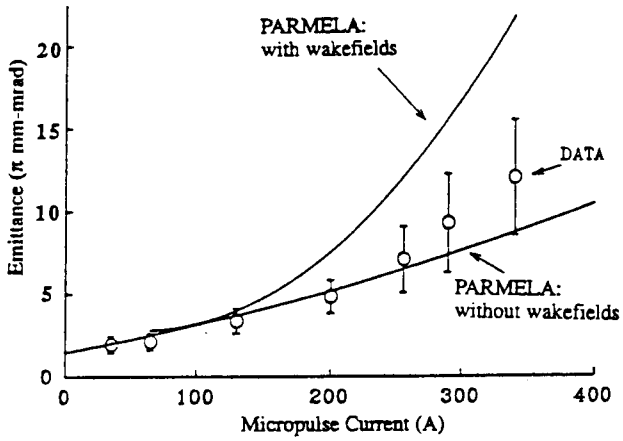

Fig. 2 APEX Emittance *vs.* Micropulse Current

that the components and the beam were properly aligned; the assumption for the upper curve was a random misalignment of components with our estimated accuracy and the beam centered between accelerators. We consider the agreement with theory to be satisfactory. Our results confirm Carlsten's theory of emittance compensation by means of solenoids[8].

Although the estimated error bars are large for emittance values measured after the 60° bend, we apparently experienced little emittance growth in the bend.

Field Emission. We found that operating with a highly polished surface on the photocathode reduces the field emission beam current by a large factor compared to operating with a machined surface.

Wakefields. Using a streak camera, we were able to directly observe the effect of transverse wakefields on the micropulse. PARMELA calculations show that the three side coupled accelerators produce appreciable transverse deflections of the beam, and, hence transverse wakefields. To compensate for these effects, the beam must be steered so that it does not pass through the geometric center of the beamline between accelerators. The streak camera technique allowed us to steer so that we could minimize the net wakefields through the total structure. A detailed description of this technique, which should prove extremely useful in tuning the beamline, is given by Wilke et. al.[9].

We plan to use the streak camera technique to measure the emittance of charge slices within the micropulse. This "slice" emittance is an important parameter in the performance of a free-electron laser.

The dependence of emittance on other parameters is discussed by Carlsten et. al.[6].

FEL Operation. Details of the APEX system's FEL operations of the system are discussed by O'Shea et. al.[10].

CONCLUSIONS

We successfully operated the Los Alamos free electron laser photoelectric injector/accelerator and beamline at its rated parameters, our experiments show that this technology is capable of producing a high-current, high-brightness beam for this and other technologies.

ACKNOWLEDGMENT

We wish to acknowledge the tireless and invaluable efforts of all those who contributed to these experiments. In particular we wish to thank S. Apgar, Paul Ortega, N. Okamoto, M. Feind, J. Barton, C. Webb, and P. Schafstall.

REFERENCES

[1] R. L. Sheffield, E. R. Gray, and J. S. Fraser,"The Los Alamos Photoinjector Program", Nucl. Instr. and Methods in Physics .**A 272** (1988) 222-226.

[2] B. E. Carlsten, L. M. Young, et. al., "Accelerator Design and Calculated Performance of the Los Alamos HIBAF Facility, "Nucl. Instr. and Methods in Physics Res.**A 296**, (1990) 687-696

[3] John C. Goldstein, Bruce E. Carlsten, and Brian D. McVey, "Inex Simulations of the Los Alamos HIBAF Free-Electron Laser MOPA Experiment," Nucl. Instr. and Methods in Physics Res.**A 296** (1990)273-281.

[4] D. W. Feldman, S. C. Bender, B. E. Carlsten,et. al., "Experimental Results From The Los Alamos FEL Photoinjector', IEEE J. Quantum Electron. **27** pp. 2636-2643, 1991

[5] J. Early, J. Barton, R. Wenzel, D. Remelius, and G. Busch, "The Los Alamos FEL Photoinjector Drive Laser", IEEE J. Quantum Electron. **27** pp. 2644-2649, 1991.

[6] Bruce E. Carlsten, Lloyd M. Young, Michael E. Jones,et. al., "Inex Design and Analysis of Experimental Performance of the Los Alamos HIBAF Facility Accelerator," IEEE J. Quantum Electron. **27** pp. 2580-2597, 1991.

[7] M. C. Ross, M. Phinney, G. Quickfall, H. Shoaee, and J. C. Sheppard,"Automated Emittance Measurements in the SLC", Proceedings of 1987 IEEE Particle Accelerator Conference, Washington, D.C. pp. 725-728

[8] Bruce E. Carlsten,"Photoelectric Injector Design Code", Proceedings of 1989 IEEE Particle Accelerator Conference, Chicago, IL, pp. 725-728

[9] M. D. Wilke, A. H. Lumpkin,P. G. O'Shea, Eric Pitcher, and R B. Feldman, "Electron-Beam Diagnostic Development for the Los Alamos FEL Facility, These proceedings.

[10]P. G. O'Shea, S. C. Bender, D. A. Byrd, et. al.,"Initial Results from the Los Alamos Photoinjector-Driven Free-Electron Laser", Nucl. Instr. and Methods inPhysics Res.**A 318** (1992) 52-57.